Study by Numerical simulation of the influence of the inclination of a cavity on the convective stability of fluid flow

M Berramdane*, M Elmir, A Missoum, J Ghouizi
ENERGARID Laboratory, Faculty of Technology, TAHRI Mohamed University, Bechar, Algeria

ABSTRACT

In this work, we present a study of natural convection in a rectangular air-filled cell with a Prandtl number Pr = 0.71 and inclined by an angle ϕ. The walls for z = 0 and z = H are impermeable and maintained at constant temperatures respectively Th and Tc, while the other two walls are impervious and adiabatic. All walls are assumed to be rigid (Figure 1). The fluid is assimilated to an incompressible Newtonian fluid whose thermo-physical characteristics are constant when the temperature difference ΔT = Th-Tc remains sufficiently low (a few degrees) for the Boussinesq approximation to remain applicable. Under these conditions, the convective flows obtained are laminar. Rayleigh is considered between $10^2 \leq Ra \leq 10^4$ for different inclinations varying from -90° to 180° of aspect ratio A=L/H=10. Our calculations highlight the influence of the angle of inclination on the triggering thresholds of natural convection, the structure of the flow and the heat transfer and thus on the convective instability.

1. INTRODUCTION

Around 1900, Henri Benard [1] by heating down a layer of thin oil observed convective cells take the form of a mosaic of regular hexagons. These cells are known as "Benard cells". As early as 1916, Lord Rayleigh [2] modeled and solved the problem of Benard, but the critical temperature obtained by Rayleigh did not correspond at all to the experimentation of Benard. Rayleigh assumed that the fluid is placed between two rigid plates while for Benard's experiment, the upper surface of the fluid is supposed to be free. Davis [3] in 1967 and Stork and Müller [4] in 1972, showed in their research that the more the cavity is confined, the higher the number of Rayleigh critical Ra_c high. At the opposite; when the lateral dimensions tend towards infinity, Ra_c tends towards a limit value equal to 1708. Schandrasekhar did a very detailed study on this number of critical Rayleigh in the book "Hydrodynamics and Hydromagnetic Stability [5]

The Boussinesq approximation allows an incompressible formulation of the Navier-Stokes equations by taking into account buoyancy forces due to the expansion of the fluid and induced by a variation of the temperature. This approximation is attributed to Boussinesq [6],

It is proposed to study two-dimensional natural convection in a stationary regime. We consider the case of rigid kinematic boundary conditions for numerical simulation. The conductive state is characterized by a zero velocity and a linear temperature profile.

*Corresponding Author: mehddi08@gmail.com

The objective of this work is the study of the influence of the angle of inclination of the enclosure on the trigger thresholds of the instability, the structure of the flow and the heat transfer.

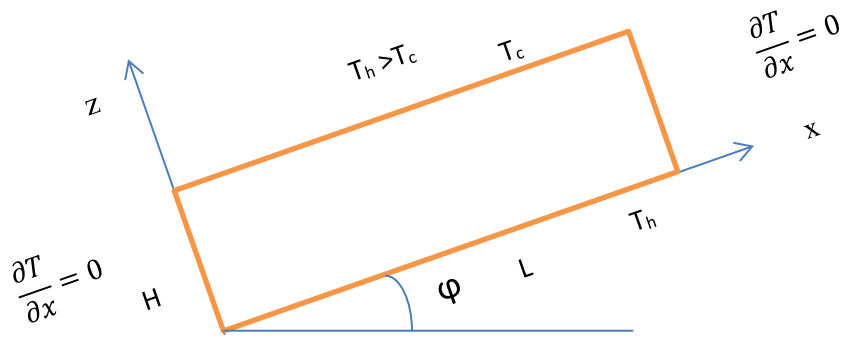

Figure 1: Physical model

2. MATHEMATICAL FORMULATION

In order to obtain a simple mathematical model, we adopt the following hypotheses:

- The flow is two-dimensional.
- The fluid is Newtonian and incompressible.
- The flow is laminar.
- Radiation heat transfer is negligible.
- Viscous dissipation is negligible in the energy equation.
- The physical properties of the fluid are constant except the density which obeys the Boussinesq approximation.
- The equations governing the flow are the conservation equations: mass, momentum and energy. Using the simplifying assumptions quoted above and taking into account the Boussinesq approximation, these equations take the following form:

$$\frac{\partial u}{\partial x} + \frac{\partial w}{\partial z} = 0 \tag{1}$$

$$u\frac{\partial u}{\partial x} + w\frac{\partial u}{\partial z} = -\frac{1}{\rho_o}\frac{\partial p}{\partial x} + \beta g(T - T_c)\sin\varphi + \nu\left(\frac{\partial^2 u}{\partial x^2} + \frac{\partial^2 u}{\partial z^2}\right) \tag{2}$$

$$u\frac{\partial w}{\partial x} + w\frac{\partial w}{\partial z} = -\frac{1}{\rho_o}\frac{\partial p}{\partial z} + \beta g(T - T_c)\cos\varphi + \nu\left(\frac{\partial^2 w}{\partial x^2} + \frac{\partial^2 w}{\partial z^2}\right) \tag{3}$$

$$u\frac{\partial T}{\partial x} + w\frac{\partial T}{\partial z} = \alpha\left(\frac{\partial^2 T}{\partial x^2} + \frac{\partial^2 T}{\partial z^2}\right) \tag{4}$$

To this system of partial differential equations are associated the following thermal and dynamic boundary conditions:

$$\text{Thermal: } \begin{cases} T(x, z = H) = Tc \ \forall x \\ T(x, z = 0) = Th \ \forall x \end{cases}$$

$$\text{Dynamic: } \begin{cases} u(x, z = H) = w(x, z = H) = 0 \ \forall x \\ u(x, z = 0) = w(x, z = 0) = 0 \ \forall x \end{cases}$$

In order to make the system of partial differential equations above dimensionless, the following reference quantities are used:

$$(x^*, z^*) = \frac{(x,z)}{H} \ ; \ (u^*, \ w^*) = \frac{H}{\alpha}(u \ , w) \ ; \ T^* = \frac{T - Tc}{Th - Tc} \ ; \ P^* = \frac{PH^2}{\rho\alpha^2}$$

We introduce these dimensionless variables in the (1)-(4) equations we obtain the following dimensionless formalism:

$$\frac{\partial u^*}{\partial x^*} + \frac{\partial w^*}{\partial z^*} = 0 \tag{6}$$

$$u^* \frac{\partial u^*}{\partial x^*} + w^* \frac{\partial u^*}{\partial z^*} = -\frac{\partial P^*}{\partial x^*} + RaPrT^* \sin\varphi + Pr\left(\frac{\partial^2 u^*}{\partial x^{*2}} + \frac{\partial^2 u^*}{\partial z^{*2}}\right) \tag{7}$$

$$u^* \frac{\partial w^*}{\partial x^*} + w^* \frac{\partial w^*}{\partial z^*} = -\frac{\partial P^*}{\partial z^*} + RaPrT^* \cos\varphi + Pr\left(\frac{\partial^2 w^*}{\partial x^{*2}} + \frac{\partial^2 w^*}{\partial z^{*2}}\right) \tag{8}$$

$$u^* \frac{\partial T^*}{\partial x^*} + w^* \frac{\partial T^*}{\partial z^*} = \frac{\partial^2 T^*}{\partial x^{*2}} + \frac{\partial^2 T^*}{\partial z^{*2}} \tag{9}$$

With the following boundary conditions:

$$\text{Thermal: } \begin{cases} T^*(x^*, z^* = 1) = 0 \ \forall x^* \\ T^*(x^*, z^* = 0) = 1 \ \forall x^* \end{cases}$$

$$\text{Dynamic: } \begin{cases} u^*(x^*, z^* = 1) = w^*(x^*, z^* = 1) = 0 \ \forall x^* \\ u^*(x^*, z^* = 0) = w^*(x^*, z^* = 0) = 0 \ \forall x^* \end{cases}$$

On the active walls of the domain, the local and average Nusselt numbers are given by the following expression:

$$Nu \ = -\left.\frac{\partial T^*}{\partial Z^*}\right|_{z^*=0} \tag{10}$$

$$Nu_a = \frac{1}{A}\int_0^A Nu \, dx^* \tag{11}$$

3. NUMERICAL SIMULATION

The finite elements method (FEM) is used in our model for discretizing the governing equations (6) to (9) along with the boundary and initial conditions. to validate our work, we compared our simulation results from A = 1 and φ=90°, with those of De Val Davis [7], Zarrit and al. [8] and Wang and al [9] in the case where $Ra=10^3$ and $Ra=10^4$. The comparison presented in Table 1 shows a very good agreement between the different works. We tested several types of mesh and we opted for a mesh consisting of 1125 elements.

Table 1: Comparison of the Nusselt numbers

Ra		$\mathbf{10^3}$	$\mathbf{10^4}$
De Val Davis [7]	Nu_a	1.117	2.238
R. Zarrit and al. [8] (FDM)		1.118	2.254
Wang and al. [9] (FEM)		1.117	2.254
Our work		1.118	2.255

4. RESULTS AND DISCUSSION

Figure 2 shows the streamlines for different inclination angles and for two distinct values of the Rayleigh number. The analysis of this figure shows that the flow is single-cell, they are manifested by co-rotating streamlines. It can be seen that there is a movement in the fluid layers as soon as the heating begins. This movement is ascending along the hot plate and descending along the cold plate. For the same value of Rayleigh number, the number of rollers decreases with the increase of the angle of inclination. As the Rayleigh number increases, the flow increases, becoming multicellular with counter-rotating rolls.

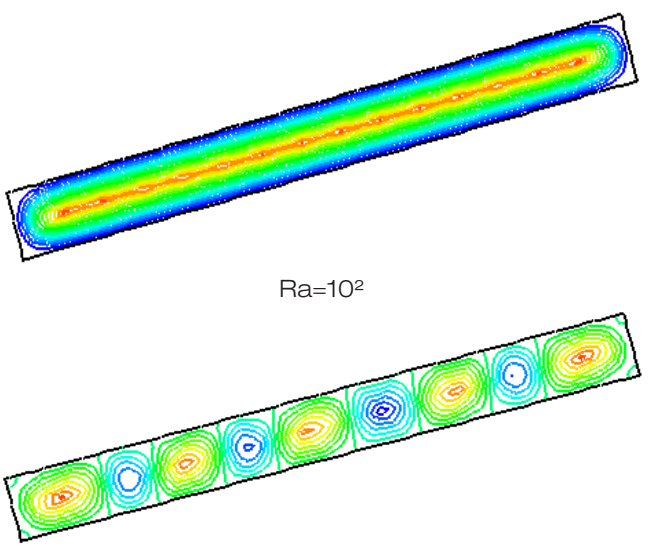

Ra=10^2

Ra=10^4

(a)

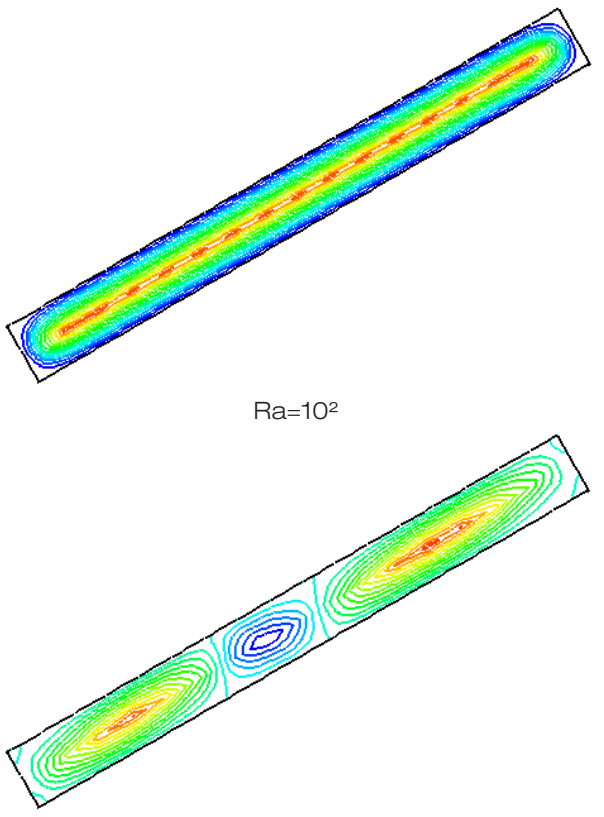

Ra=10^2

Ra=10^4

(b)

Figure 2: Streamlines for (a) φ=15° and (b) φ=30°

Figure 3 represents the variations of the maximum streamline function as a function of φ for different values of Ra, and Figure 4 represents the variations of the maximum streamline function as a function of Ra for different values of φ. For Ra < 300, the inclination has no influence on the fluid flow giving a value of zero at $|\psi|_{Max}$. For the other values of Ra, it increases with the increase of φ and reaches a maximum value for a vertical cavity (φ=90°). The intensity of the flow increases with the inclination. Indeed, the values of $|\psi|_{Max}$ increases with increasing tilt angle of the cavity pour Ra = 10^4 (See Table 2)

Table 2: Influence of $|\psi|_{Max}$ on φ

φ	**0°**	**30°**	**60°**	**90°**
$\|\psi\|$Max	08.03	11.53	18.04	20.10

Figure 5 shows isotherms for Ra = 1708 and different values of inclination. For a horizontal cavity, the transfer is almost conductive thus giving a stratification. For the other angles, this stratification disappears as one increases the angle of inclination giving rise to the convective heat transfer.

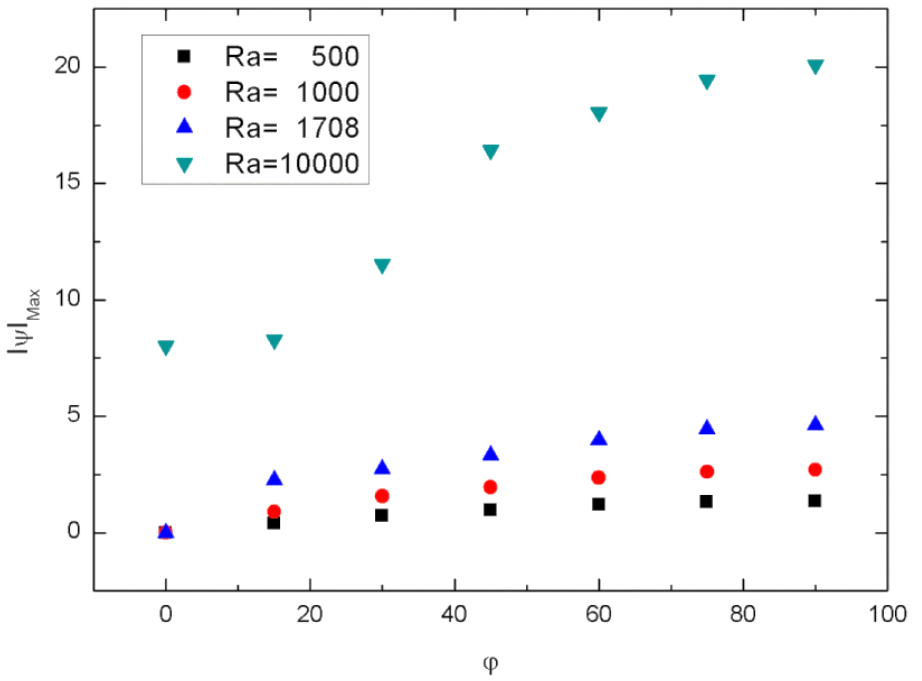

Figure 3: Variation of maximal streamline function according to φ

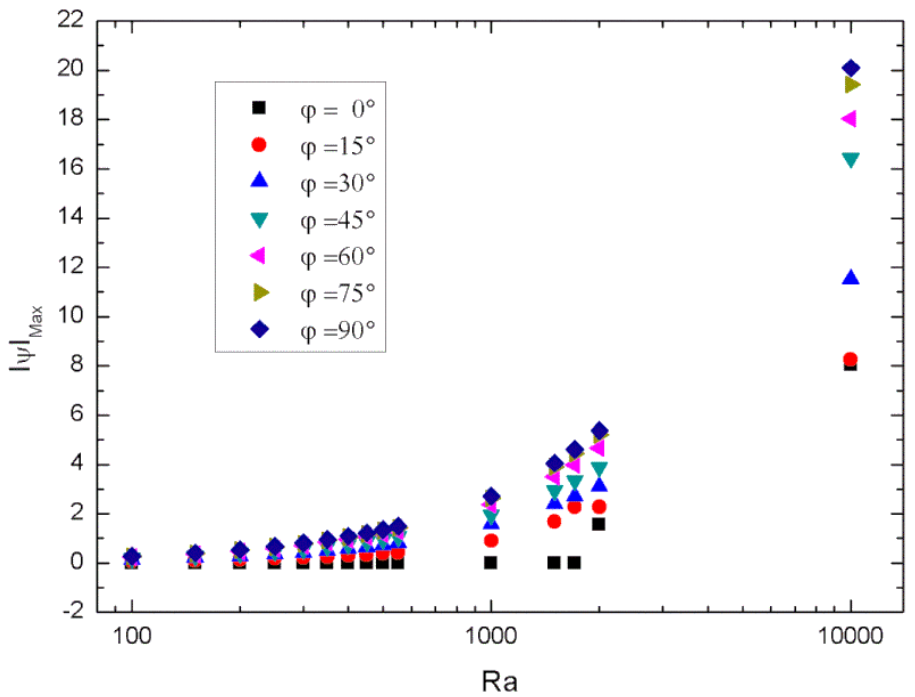

Figure 4: Variation of maximal streamline function according to Ra

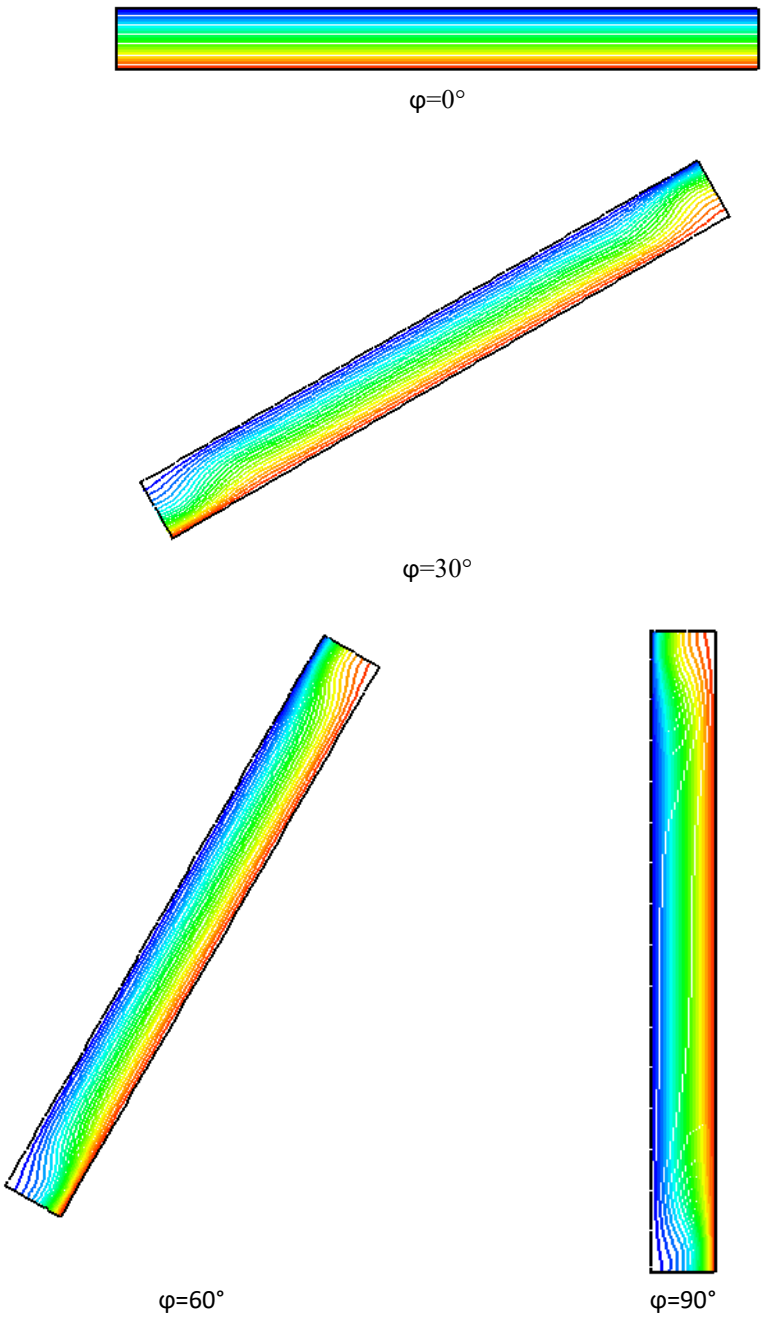

Figure 5: Isotherms for Ra=1708

Figure 6 represents the variations of the average Nusselt number as a function of φ for different values of Ra, The evolution of average Nusselt number as a function of Rayleigh

number is shown in Figure 7. By analyzing the variation of the Nusselt number as a function of the angle of inclination, it is found that the heat transfer is greater for the strong inclinations and less important for the low inclinations. For high Rayleigh number, the Nusselt number decreases with increasing value of the tilt angle. This decrease is due to the deceleration of the flow near the active walls. In the purely conductive case it will be noted that the average Nusselt number is equal to the unit. We can say that by increasing the angle of inclination, the triggering of the instability will start for Rayleigh number values lower than that found for the Rayleigh-Bénard configuration (Table 3). We can also notice that the positive and negative angles take the same critical Rayleigh value.

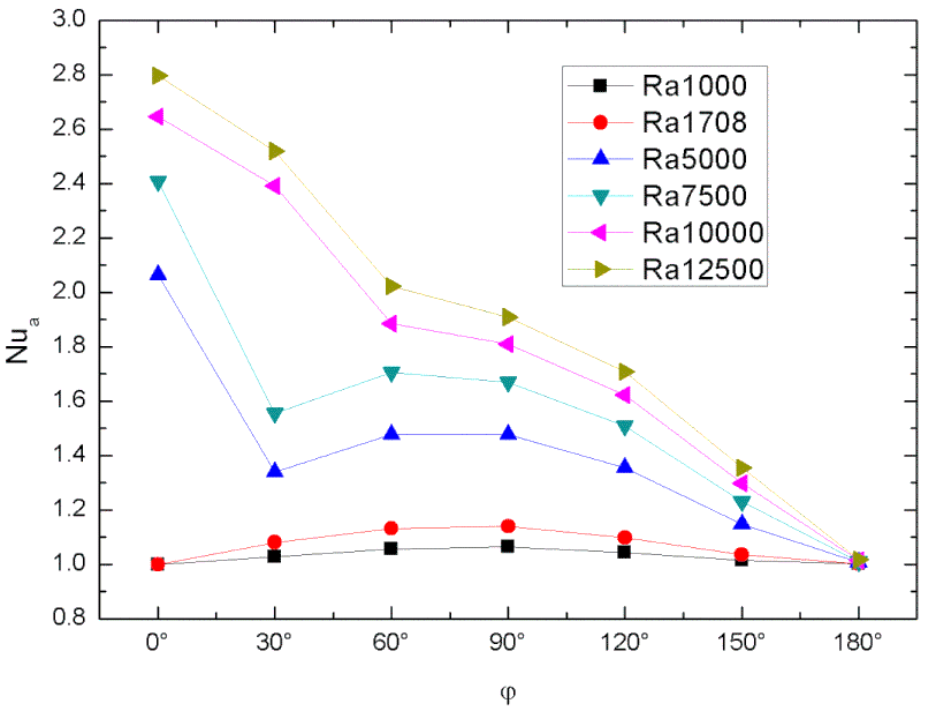

Figure 6: Variation of the average Nusselt number according to the angle of inclination

Table 3: Critical Rayleigh number vs tilt angle

φ	**0°**	**±15°**	**±30°**	**±45°**	**±60°**	**±75°**	**±90°**
Ra_c	1740	950	550	450	350	300	300

Figure 8 shows the evolution of the number of critical Rayleigh number as a function of the angle of inclination for a heating of the cavity from below. For positive values of φ, the Ra_c increases exponentially while for negative values we find the opposite phenomenon. We propose in this study a correlation between the critical Rayleigh and the angle of inclination given by the following relation:

$$Ra_c = ae^{-\frac{\varphi}{b}} + c \quad (12)$$

Table 4: Proposed correlation between the critical Rayleigh and the angle of inclination (Equation 12).

a	b		c	R^2
	φ <0	φ >0		
1453.70	-18.73	18.73	287.35	0.998

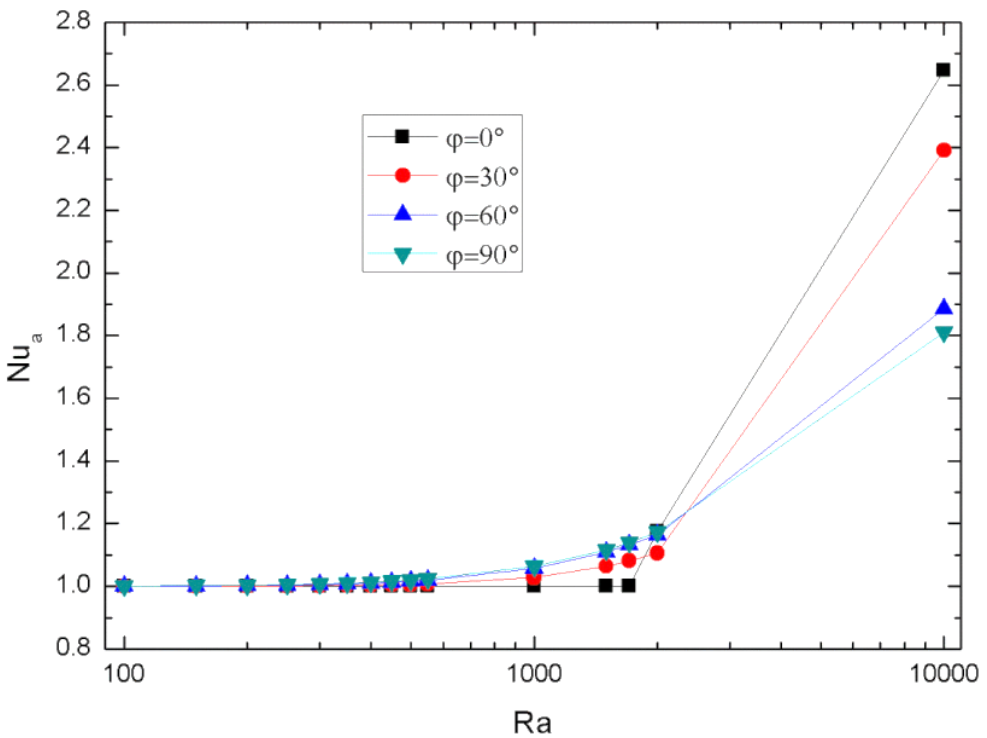

Figure 7: Variation of the average Nusselt number according to the Rayleigh number

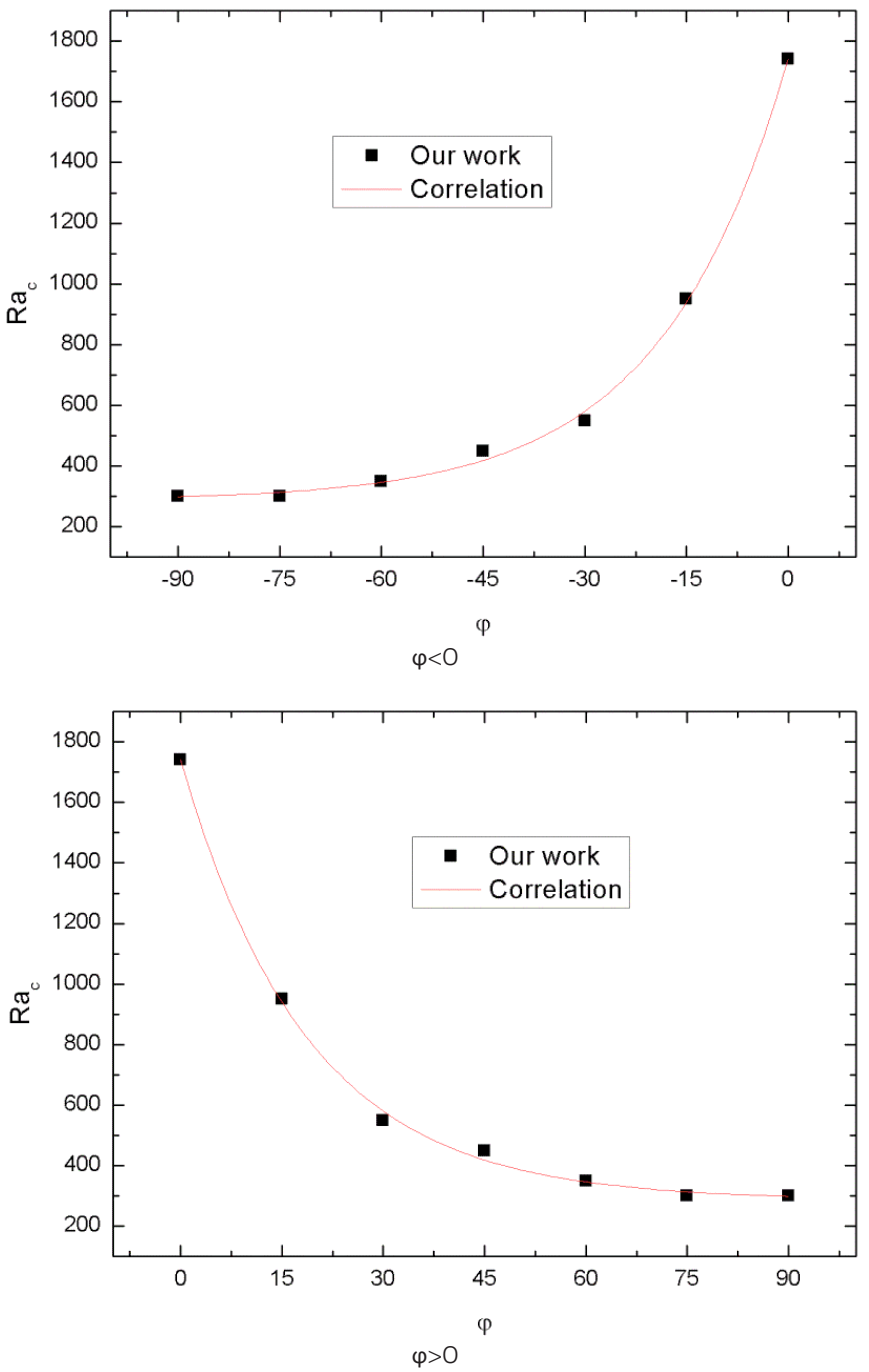

Figure 8: Variation of the Critical Rayleigh number according to the tilt angle

5. CONCLUSION

We performed a two-dimensional numerical study of natural convection coupled heat transfer in a Rayleigh-Bénard inclined rectangular cavity. We examined the effect of inclination angle on dynamic flow field and on heat transfer. The results showed that for large numbers of Rayleigh, convective heat transfer becomes increasingly low and leads to a decrease in the rate of heat transfer as the angle of inclination increases. The critical Rayleigh number decreases with increasing angle of inclination. A correlation between the critical Rayleigh number and the angle of inclination has been determined. Positive values of the angle of inclination accelerate the appearance of convection against negative values of this angle delay the appearance of convection.

REFERENCES

[1] H. Bénard, Les tourbillons cellulaires dans une nappe liquide, Revue Générale des Sciences Pures et Appliquées, Vol. 11, pp. 1261-1271 et 1309-1328 (1900).

[2] Lord Rayleigh, On convective currents in a horizontal layer of fluid when the higher temperature is on the underside, Scientific Papers. Cambridge University Press. Vol. 6, pp. 432-446 (1920).

[3] S. Davis, Convection in a Box, Linear Theory, J. Fluid Mech., Vol. 30, No..3, pp. 465-478 (1967).

[4] K. Stork and U. Müller, Convection in boxes: Experiments J. Fluid Mech., vol. 54, part 4, pp. 599-611 (1972).

[5] S.Chandrasekhar, Hydrodynamic and Hydromagnetic Stability, Oxford Clarendon Press, London, pp.9-73, (1961)

[6] J. Boussinesq, Théorie analytique de la chaleur, Vol. 2, Gauthier-Villars, Paris, 1903.

[7] G. de Vahl Davis, 'Natural Convection of Air in a Square Cavity: A Bench Mark Numerical Solution', International Journal for Numerical Methods in Fluids, Vol. 3, No. 3, pp. 149 – 164, 1983

[8] R.Zarrit et al. convection naturelle dans une cavité rectangulaire incliné de différents de forme, Revue des Energies Renouvelables Vol.19, No. 1 (2016) 97-109

[9] H. Wang and M.S. Hamed, 'Flow Mode-Transition of Natural Convection in Inclined Rectangular Enclosures Subjected to Bidirectional Temperature Gradients', International Journal of Thermal Sciences, Vol. 45, No. 8, pp. 203 - 217, 2006.